

Catalytic Conversion of Methane and Propylene to 1-Butene

Jack H. Lunsford,* Michael P. Rosynek, C. Edwin Smith, Mingting Xu, and Zhenqiang Yu

Department of Chemistry, Texas A&M University, College Station, Texas 77843

Received: April 3, 1995; In Final Form: June 13, 1995*

The oxidative cross-coupling of methane with propylene has been studied over several catalysts. A material containing 1.9 wt % Mn and 5 wt % NaCl on SiO₂ was found to be the most effective for this reaction. At 650 °C, it was possible to attain selectivities to 1-butene and butadiene of 57% and 8.0%, respectively, at a propylene conversion of 38%. Experiments utilizing ¹³CH₄ confirm that methane was indeed involved in the formation of the C₄ products. Methyl radicals derived from CH₄ and allyl radicals derived from C₃D₆ were simultaneously detected over the catalysts using a matrix isolation electron spin resonance method. These surface-generated radicals enter the gas phase, where most of the coupling is believed to occur. In addition to the cross-coupling reaction, methyl radicals couple to form ethane, and allyl radicals couple to form 1,5-hexadiene. The latter hydrocarbon reacts extensively back to propylene over the catalysts at 650 °C.

Introduction

The oxidative coupling of methane with other organic molecules has greatly expanded the potential for the utilization of methane to produce more valuable chemicals. The most extensively studied of these reactions has been the oxidative coupling of methane with toluene to form ethylbenzene and subsequently styrene.^{1–6} Ruckenstein and Khan⁷ have recently reported on the coupling of methane with acetonitrile to form propionitrile and acrylonitrile.

Since many of the same oxides are capable of forming CH₃[•] radicals from CH₄ and C₃H₅[•] radicals from C₃H₆, it is expected that an effective catalyst could be found to produce butenes via a coupling reaction. Ideally, one would like to form isobutylene because of its economic importance; however, this is an unlikely product of the cross-coupling reaction since the unpaired electron in the allyl radical resides largely on the terminal carbon atoms.⁹ Sofranko *et al.*¹⁰ demonstrated that the addition of propylene during the oxidative coupling of methane in a cyclic mode resulted in the formation of C₄ hydrocarbons, while simultaneously suppressing the formation of C₂ products. They speculated that CH₃[•] radicals reacted with C₃H₆ to form C₄H₉[•] radicals, which was followed by the loss of H[•] to generate *n*-butenes. Sodesawa *et al.*¹¹ found that in a continuous flow system PbO/Al₂O₃, La₂O₃, and Na₂O/La₂O₃ catalyzed the cross-coupling of CH₄ with C₃H₆ to produce butene and butadiene. The Na₂O/La₂O₃ catalyst was the most effective, giving a 10% yield of C₄ compounds. In the work of Sodesawa *et al.*, there was little evidence for a particular reaction mechanism, and one must be concerned with the possibility that the C₄ products came almost exclusively from the cracking of 1,5-hexadiene. That is, allyl radicals may first couple, and the resulting hexadiene may then subsequently crack, resulting in no actual incorporation of CH₃[•] radicals into the observed C₄ hydrocarbons.

The present study was performed in order to more fully establish the origin of the butene and butadiene products in the CH₄/C₃H₆ cross-coupling reaction. ¹³CH₄ and ¹²C₃H₆ were reacted in the presence of oxygen over several catalysts, and the ¹³C distribution in the products was determined. In addition, the simultaneous formation of surface-generated gas-phase methyl and allyl radicals was followed over both good and poor

cross-coupling catalysts. The results demonstrate that the C₄ products are indeed a result of the cross-coupling reaction and that the coupling may occur between radicals in the gas phase. It was shown that a NaCl–Mn/SiO₂ catalyst is quite effective for this reaction. Combined butene and butadiene yields of up to 36% can be achieved, based on the conversion of propylene.

Experimental Section

Reagents and Catalysts. Methane (99.9%, UHP), oxygen (99.9%, extra dry), and propylene (polymer grade) were obtained from Matheson. A Matheson certified gas mixture containing 10% Ar/He was used as an internal standard. 1,5-Hexadiene (99.9%) was obtained from Aldrich. The ¹³C-labeled methane (99.9%) and propylene-*d*₆ (98%) were purchased from Cambridge Isotope. All of the gases were used without further purification.

A conventional 5 wt % Li/MgO catalyst was prepared by adding Li₂CO₃ to deionized water at 50 °C under vigorous stirring. A Li⁺–MgO–Cl[–] catalyst was prepared by adding aqueous HCl to a slurry of MgO, followed by the addition of a solution of LiNO₃.¹² The atomic ratio of Li/Mg/Cl in the resulting catalyst was 0.44:1:0.42, based on ICP analysis. The MgO-supported bialkali metal chlorides and hydroxides, including (5 mol % LiCl + 5 mol % NaCl)/MgO, (5 mol % LiOH + 5 mol % NaOH)/MgO, (5 mol % NaCl + 5 mol % CsCl)/MgO, and (5 mol % NaOH + 5 mol % CsOH)/MgO catalysts, were prepared according to the method of Ruckenstein and Khan.¹³ Briefly, an aqueous solution containing the two metal salts or hydroxides was introduced into an aqueous slurry of MgO at 80 °C. The solution was evaporated to dryness, and the catalysts were heated overnight at 120 °C. All of the above catalysts were calcined in air at 750 °C for *ca.* 15 h and were pretreated in flowing O₂ for 2 h prior to use. The 1.9 wt % Mn–5 wt % NaCl/SiO₂ catalyst was prepared from Mn(NO₃)₂, NaCl, and SiO₂ (Davison grade 57) by aqueous impregnation. An appropriate amount of SiO₂ was added to a solution containing the desired amount of Mn(NO₃)₂ and NaCl. After evaporation to dryness, the catalyst was heated overnight at 120 °C and calcined in air at 750 °C for 4 h. The apparent densities and the surface areas of the prepared catalysts are given in Table 1.

Reaction System. Catalytic results were obtained both in a single-pass flow mode and in a continuous recycle mode. All of the single-pass flow experiments were carried out in an

* Abstract published in *Advance ACS Abstracts*, August 1, 1995.

TABLE 1: Apparent Density and Surface Areas of Catalysts

catalysts	apparent density, g/mL	surface area, m ² /g
Sr/La ₂ O ₃	1.11	7.8
Li/MgO	1.14	2.5
Li ⁺ -MgO-Cl ⁻	0.92	1.6
(LiOH + NaOH)/MgO	0.40	11.2
(LiCl + NaCl)/MgO	0.35	5.1
(NaOH + CsOH)/MgO	0.73	4.9
(NaCl + CsCl)/MgO	0.66	3.6
NaCl-Mn/SiO ₂	0.45	7.8

alumina downflow reactor having an internal diameter of 10 mm. Quartz chips filled the space above the catalyst bed and served to preheat the reaction gases. Product gases were analyzed using a Hewlett-Packard Model 5890II gas chromatograph containing 13X molecular sieve and Haysept S packed columns. A Matheson certified gas mixture containing CO, CO₂, CH₄, C₂H₄, C₂H₆, C₃H₆, C₃H₈, C₄ isomers, 1-pentene, and 1,5-hexadiene was used to calibrate the GC.

A recirculation system, which has been described previously,¹⁴ was used to determine the ¹³C distribution in the products when ¹³CH₄ was a reagent. ¹³CH₄ was first introduced to an isolated volume. A recirculating pump was used to mix this gas with a previously prepared reagent gas mixture. After circulating the gases over the catalyst for a fixed period, they were introduced via a sample loop into a GC/MS instrument. The GC/MS analysis was performed using a Hewlett-Packard 5890II gas chromatograph, equipped with a Model 5971 mass sensitive detector. A Haysept S column was used for the separation of the gas components. Unless otherwise stated, the selectivities were calculated from the ratio of the moles of C₃H₆ converted to a particular product to the total number of moles of C₃H₆ reacted.

Radical Detection. A matrix isolation electron spin resonance (MI-ESR) system¹⁵ was used to detect gas phase radicals that emanate from the surface. In a typical experiment, a gas mixture containing hydrocarbons, oxygen, and argon was passed over the catalyst at a pressure of *ca.* 1 Torr, and the effluent entered a differentially pumped region. The gases, including any radicals that may have been formed, were frozen in an argon or carbon dioxide matrix on a sapphire rod at 15 K. Following a collection period of 25 min, the rod was lowered into a microwave cavity, and the spectrum of the radicals was obtained by ESR spectroscopy. By a suitable deconvolution of the spectra and double integration, the relative concentrations of the various radical species were determined. The gas flow rates at STP were CH₄/C₃H₆ or C₃D₆/O₂ = 1.1/0.073/0.013 mL/min. The Ar or CO₂ flow rate was 3.8 mL/min. All reactions were carried out at 650 °C over 200 mg of catalyst.

TABLE 2: Comparison of the Catalytic Performance over Quartz Chips and Catalysts in the Oxidative Coupling of Methane and Propylene^a

catalyst	conversion, %			selectivity, %							
	C ₃ H ₆	CH ₄	O ₂	CO	CO ₂	C ₂ H ₄	C ₂ H ₆	1-butene	butadiene	C ₅ ^b	C ₆ ^b
quartz chips	1.4	0.5		43	57						
Sr/La ₂ O ₃	29	1.0	85	23	46	5.4	8.9	12	4.2	0.0	0.0
Li/MgO	35	5.4	81	1.2	36	10	9.0	32	5.1	2.1	3.5
Li ⁺ -MgO-Cl ⁻	22	4.1	57	7.0	23	8.7	5.8	44	5.6	0.0	6.2
(LiCl + NaCl)/MgO	21	3.6	63	7.4	9.7	11	3.3	56	6.9	0.0	5.2
(LiOH + NaOH)/MgO	30	3.5	76	5.9	34	6.5	6.3	36	5.6	0.0	6.1
(NaCl + CsCl)/MgO	24	3.7	66	6.0	7.1	17	5.3	52	6.7	0.0	6.1
(NaOH + CsOH)/MgO	31	4.1	78	6.5	24	10	8.5	37	6.8	0.0	6.8
NaCl-Mn/SiO ₂	65	11	95	12	17	9.6	5.7	47	6.9	0.0	0.8
NaCl-Mn/SiO ₂ ^c	38	4.0	66	7.2	4.8	8.8	5.2	57	8.0	0.0	8.1

^a Reaction temperature = 650 °C; volume of the catalyst = 1 mL; flow rate = 60 mL/min; *P*(CH₄) = 504 Torr, *P*(C₃H₆) = 48 Torr, *P*(O₂) = 42 Torr; balance: helium; data taken after 2 h on stream. ^b C₅ = *n*-pentene; C₆ = 1,5-hexadiene. ^c Volume of the catalyst = 0.3 mL (0.15 g).

Results and Discussion

Comparison of Catalytic Performance. The results obtained over quartz chips and over the catalysts used in this study are summarized in Table 2. The catalysts were chosen because they have been shown to be effective in the cross-coupling of methane with toluene and/or the oxidative coupling of methane.^{6,12,13,16-18} The conditions employed here, particularly the temperature, may not be the optimum for each of the catalysts in other types of coupling reactions. Because CH₄ is much less reactive than C₃H₆, a large CH₄/C₃H₆ ratio was used. The results reported in Table 2 were obtained at a residence time of 1 s and after 2 h on stream. As will be discussed subsequently, some of the catalysts reached steady state after this period, but others did not.

With only quartz chips in the reactor, the CH₄ and C₃H₆ conversions were small, and only CO_x was observed as a product. All of the catalysts studied, with the exception of Sr/La₂O₃, were effective in the conversion of C₃H₆ and CH₄; however, the total moles of C₃H₆ converted were less than those of CH₄. After 2 h on stream, the best C₄ selectivities were obtained with the (LiCl + NaCl)/MgO, the (NaCl + CsCl)/MgO, and the NaCl-Mn/SiO₂ catalysts. Khan and Ruckenstein⁶ similarly found that the former two catalysts were among the best that they tested for the cross-coupling of methane and toluene. Whereas they found that the catalysts prepared from the mixed alkali metal hydroxides had about the same favorable performance, we observed that the hydroxide-derived catalysts were considerably less selective in the case of the CH₄/C₃H₆ reaction, although the C₃H₆ conversion levels were somewhat greater. It should be noted that Khan and Ruckenstein obtained their results at 750 °C. In terms of overall C₄ yield, the NaCl-Mn/SiO₂ catalyst was superior. A C₄ yield of 35% was attained under the conditions stated in Table 2, based on the amount of C₃H₆ converted. A C₄ selectivity of 65% was attained at a C₃H₆ conversion of 38% over the NaCl-Mn/SiO₂ catalyst. The conversion of CH₄ and the C₄ yield obtained over the Sr/La₂O₃ catalyst were small, considering the effectiveness of this catalyst in the oxidative coupling of CH₄, albeit at a temperature of 800 °C.

The hydrocarbon distributions shown in Table 2 are about what one would expect from normal coupling and cross-coupling reactions. The C₄ products consisted primarily of 1-butene and butadiene, with less than 5% 2-butenes. The butadiene is derived from the oxidative dehydrogenation of 1-butene. The 1,5-hexadiene is indicative of allyl radical coupling. The C₂ products suggest CH₃^{*} radical coupling, although it will be shown subsequently that C₂H₄ is derived mainly from the cracking of 1,5-hexadiene.

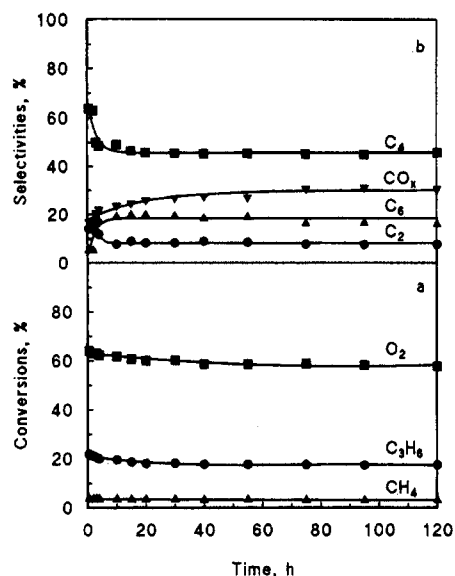


Figure 1. Variation in (a) conversion and (b) selectivity with time on stream at 650 °C over the (LiCl + NaCl)/MgO catalyst: the flow rates for CH₄, C₃H₆, O₂, and He were 39, 3.8, 3.4, and 13 mL/min, respectively.

Effect of Reaction Conditions on Conversion and Product Distribution. Variations in the conversions and selectivities during prolonged times on stream were determined for the Li/MgO, (LiCl + NaCl)/MgO, and NaCl-Mn/SiO₂ catalysts. At 650 °C, no changes were observed in the conversions or selectivities over a period of 120 h for the Li/MgO catalyst and 50 h for the NaCl-Mn/SiO₂ catalyst. By contrast, the C₄ selectivity over the (LiCl + NaCl)/MgO catalyst decreased for a period of *ca.* 15 h, while the 1,5-hexadiene selectivity simultaneously increased as shown in Figure 1. These results suggest that the catalyst may have become progressively less effective in the generation of CH₃[•] radicals, resulting in more extensive coupling of allyl radicals. Alternatively, the same sites that were responsible for the generation of allyl radicals may also have catalyzed the cracking of 1,5-hexadiene and may have become increasingly poisoned during time on stream. The latter explanation is more consistent with the decrease in C₃H₆ conversion over the same 15 h period. As a result of these changes, the steady state C₄ yield of the (LiCl + NaCl)/MgO catalyst became comparable to that of the Li/MgO catalyst.

Since the Li/MgO and NaCl-Mn/SiO₂ catalysts were stable with respect to time on stream, additional experiments were performed on these two materials to determine the conditions needed to maximize C₄ selectivity and yield. In addition, results were also obtained for the oxidative coupling of the two hydrocarbon reagents separately and for the reaction of 1,5-hexadiene.

The effect of residence time on catalytic performance is summarized in Table 3. These data were obtained by proportionally increasing the flow rate of each reagent; therefore, the partial pressures of the hydrocarbons remained constant. As expected, the conversions increased with increasing residence time, but not in a linear manner because the O₂ conversion became limiting at larger residence times. At a residence time of 0.5 s, the conversion over the NaCl-Mn/SiO₂ catalyst was considerably greater than that over the Li/MgO catalyst. The apparent densities and surface areas of the two catalysts (Table 1) were such that the available surface in 1 mL of each catalyst was approximately the same. Over a range of residence times, the C₄ and CO_x selectivities varied slightly with the Li/MgO catalyst. The effect of residence time on C₄ and CO_x selectivities was considerably greater over the NaCl-Mn/SiO₂ catalyst.

TABLE 3: Effect of Residence Time on the Distribution of Products^a

residence time ^a	conversion, %			selectivity, %					
	C ₃ H ₆	CH ₄	O ₂	CO _x	C ₂	C ₄	C ₅	C ₆	
Li/MgO									
0.5	29	3.0	65	35	21	37	0.0	6.5	
0.7	33	3.3	70	38	17	38	1.8	5.8	
1.1	35	4.1	79	38	18	38	1.9	3.7	
1.8	48	3.7	92	40	24	31	2.1	1.6	
NaCl-Mn/SiO ₂									
0.3	42	5.3	75	19	13	63	0.0	4.5	
0.5	45	6.2	78	20	17	61	0.0	2.7	
0.7	53	8.7	85	23	19	57	0.0	0.8	
1.1	66	11	93	25	22	52	0.0	0.1	
1.5	69	11	95	32	21	48	0.0	0.0	
1.8	71	11	96	37	22	41	0.0	0.0	

^a Reaction temperature = 650 °C; CH₄:C₃H₆:O₂ = 11:1:0.9; residence time was varied by changing the total flow rate while keeping the partial pressures of the hydrocarbons constant. Volume of catalyst = 1 mL.

TABLE 4: Effect of Reaction Temperature on the Distribution of Products^a

temp, °C	conversion, %			selectivity, %					
	C ₃ H ₆	CH ₄	O ₂	CO _x	C ₂	C ₄	C ₅	C ₆	
Li/MgO									
600	25	2.9	27	50	11	23	0.0	16	
625	26	4.7	57	43	13	34	0.0	9.6	
650	35	5.4	81	38	19	37	2.1	3.5	
675	44	5.7	94	35	25	37	2.7	0.0	
700	44	6.3	94	32	26	40	2.6	0.0	
NaCl-Mn/SiO ₂									
600	27	1.1	19	49	8.3	15	0.0	27	
625	44	5.8	64	35	10	43	0.0	12	
650	66	10	93	29	16	56	0.0	0.0	
675	70	11	98	25	22	53	0.0	0.0	
700	71	11	99	21	27	52	0.0	0.0	
725	72	12	100	22	29	49	0.0	0.0	
750	72	12	100	21	36	43	0.0	0.0	

^a Volume of the catalyst = 1 mL; P(CH₄) = 504 Torr, P(C₃H₆) = 48 Torr, and P(O₂) = 42 Torr; flow rate = 60 mL/min; balance = helium.

Over both catalysts, the 1,5-hexadiene selectivity decreased significantly with increasing residence time, indicating that this hydrocarbon undergoes secondary reactions (see below).

The effect of reaction temperature on the conversion and product distribution over the Li/MgO and NaCl-Mn/SiO₂ catalysts is summarized in Table 4. As is characteristic of oxidative coupling, both the conversion and the selectivity to the desired product increase with reaction temperature up to some optimum point. The enhanced selectivity results from the fact that radical coupling reactions are second-order in radical concentration, while the radical destruction reactions are first-order. At higher temperatures, the rate of radical formation is greater, resulting in improved selectivities. This is not the case, however, for the selectivity of 1,5-hexadiene because of rapid secondary reactions at these temperatures. The favorable effect of temperature on C₄ yield over Li/MgO suggests that even higher temperatures would be desirable, but this is not practical because lithium is rapidly lost from the catalyst at T > 700 °C.¹⁹ Over the NaCl-Mn/SiO₂ catalyst, the C₄ selectivity reached a maximum value of 56% at 650 °C. At higher temperatures, the O₂ was almost completely consumed, and no additional butene and butadiene could be formed. The slight loss in C₄ selectivity at T > 650 °C probably reflects the thermal cracking of the C₄ products to C₂H₄. The CO_x selectivity actually decreased at temperatures above 675 °C.

TABLE 5: Effect of CH₄/C₃H₆ Ratio on the Distribution of Products over a Li/MgO Catalyst^a

CH ₄ /C ₃ H ₆	conversion, %			selectivity, %				
	C ₃ H ₆	CH ₄	O ₂	CO _x	C ₂	C ₄	C ₅	C ₆
4.5	20	4.6	93	38	14	33	1.5	13
8.2	27	5.0	84	38	16	38	2.0	6.1
11	35	5.4	81	38	19	37	2.1	3.5
16	37	4.8	75	37	24	35	2.4	2.2

^a Reaction temperature = 650 °C; volume of the catalyst = 1 mL; flow rate = 60 mL/min; $P(\text{CH}_4) = 504$ Torr, $P(\text{O}_2) = 42$ Torr; balance = helium.

TABLE 6: Propylene Oxidation or the Oxidative Coupling of Methane over Li/MgO and NaCl–Mn/SiO₂ Catalysts^a

partial press. of reagent, Torr	conversion, %		selectivity, %					
	reagent	O ₂	CO _x	C ₂ H ₄	C ₂ H ₆	C ₄	C ₅	C ₆
Li/MgO								
C ₃ H ₆								
32	45	88	62	9.4	0.2	15	0.0	13
48	39	95	57	9.3	0.7	16	0.0	17
61	33	96	54	9.6	1.1	17	0.0	19
112	26	100	49	10	2.6	20	0.0	19
CH ₄								
504	4.6	76	26	9.8	64			
NaCl–Mn/SiO ₂								
C ₃ H ₆								
48	33.4	54	36	8.0	0.0	8.7	0.0	47
CH ₄								
504	6.1	78	18	19	63	0.4		

^a Except for the hydrocarbon reagents, reaction conditions were the same as those in Table 4.

The CH₄/C₃H₆ ratio was varied by keeping the pressures of CH₄ and O₂ constant at 504 and 42 Torr, respectively, and decreasing the partial pressure of propylene from 112 to 32 Torr. As indicated by the results of Table 5, the CH₄ conversion remained nearly constant, but the percent conversion of C₃H₆ increased with increasing CH₄/C₃H₆ ratio (*i.e.*, decreasing C₃H₆ partial pressure). The C₄ selectivity remained nearly constant, while the 1,5-hexadiene selectivity decreased with decreasing partial pressure of C₃H₆ and the C₂ selectivity increased. These results indicate that at high C₃H₆ partial pressure (small CH₄/C₃H₆ ratios) the allyl radical coupling competes favorably with the cross-coupling reaction, and at large CH₄/C₃H₆ ratios the CH₃[•] radical coupling competes in a similar manner.

For comparison, the oxidative coupling of propylene, in the absence of methane, was carried out under the same conditions as were used to obtain the results of Table 5. The results are given in Table 6. As expected, the selectivity for 1,5-hexadiene increased with increasing C₃H₆ pressure. Since the 1,5-hexadiene does not significantly crack to C₄ products (see below), the origin of the butene and butadiene is uncertain. Only a few CH₃[•] radicals were detected when C₃H₆ and O₂ reacted over the catalysts; thus, it is unlikely that any secondary cross-coupling occurred. When CH₄ was the only hydrocarbon reagent, C₂H₆ was the principal hydrocarbon product; trace amounts of C₃ and C₄ were detected.

Additional information about the secondary reactions of 1,5-hexadiene was obtained from experiments in which only 1,5-hexadiene and oxygen were reagents. The resulting hydrocarbon products were analyzed by GC, using a FID detector. A Cl⁻/Al₂O₃ capillary column was used to separate the components. As shown by the results of Table 7, the 1,5-hexadiene began to react at a temperature of only 450 °C, and at 650 °C more than 85% of the reagent had reacted, even over quartz chips (results not shown). The product distribution, however, was different over the quartz chips and the catalysts. Over the

TABLE 7: Oxidation of 1,5-Hexadiene over Li/MgO and NaCl–Mn/SiO₂ Catalysts^a

temp, °C	conversion, %	distribution of hydrocarbons, % ^b						
		CH ₄	C ₂ H ₄	C ₂ H ₆	C ₃ H ₆	C ₄	C ₅	C ₆
Li/MgO								
450	1.3	0.0	27	0.0	26	0.0	47	0.0
500	8.2	0.3	18	1.8	30	0.3	47	2.6
550	18	0.7	16	1.1	34	2.4	21	4.5
600	48	1.1	13	0.4	53	0.8	17	15
650	87	1.5	11	0.4	53	1.0	13	20
NaCl–Mn/SiO ₂								
450	4.3	0.7	24	5.7	27	2.3	40	1.3
500	13	1.2	16	11	29	1.8	38	2.2
550	22	1.3	15	16	41	1.6	20	5.1
600	56	0.9	9.8	26	44	1.1	11	7.8
650	95	1.1	6.3	26	48	0.8	7.8	10

^a Volume of the catalyst = 1 mL; $P(\text{O}_2) = 42$ Torr, $P(\text{C}_6\text{H}_{10}) = 42$ Torr; $\text{N}_2:\text{C}_6\text{H}_{10}:\text{O}_2 = 10:1:1$. ^b C₄ = 1-butene and butadiene; C₅ = *n*-pentene and *n*-pentane; C₆ = benzene and C₆ olefins.

quartz chips, 1-butene and butadiene were significant products, but over the catalysts almost no 1-butene and butadiene was produced, which confirms that under oxidative coupling conditions the C₄ products were not derived from the cracking of 1,5-hexadiene. Over the two catalysts, the major product at 650 °C was C₃H₆. Thus, in the cross-coupling experiments described above, much larger amounts of 1,5-hexadiene may have been formed, but it would have reacted back to C₃H₆ and, to a lesser extent, C₂H₄ and C₅ products. The major difference in product distributions over the two catalysts was the percentage of C₂H₄ and C₂H₆. With the NaCl–Mn/SiO₂ catalyst much more C₂H₆ than C₂H₄ was formed from the 1,5-hexadiene, whereas the reverse was true with the Li/MgO catalyst. The mechanism by which C₂H₆ was formed is not obvious.

Isotopic Experiments. Experiments were performed in the recirculating reactor by cofeeding ¹³CH₄, normal propylene, and oxygen. Thus, the amount of ¹³C in a particular product revealed the extent to which CH₄ was involved in the formation of that product. Of particular interest was the isotopic distribution in the C₄ products. If the 1-butene and the butadiene were formed via the cross-coupling reaction, each C₄ molecule would have a single ¹³C atom. The composition of ¹³C, other than the natural abundance, in the total C₄ products is defined as

$$[P(^{13}\text{C}_4)/P(^{12}\text{C}_4 + ^{13}\text{C}_4)] \times 100\%$$

From the GC/MS spectrum, it is possible to distinguish C₄ molecules containing 0, 1, or 2 ¹³C atoms.

Using this technique, the ¹³C distribution in the products was determined following the reaction of ¹³CH₄ and C₃H₆ over Li/MgO at 650 °C. The C₃H₆ pressure was varied, while the ¹³CH₄ pressure was kept constant at 252 Torr. As shown in Table 8, the percentage of C₄ product molecules containing one ¹³C atom increased from 38% to 69% as the ¹³CH₄/C₃H₆ ratio increased from 1.8 to 14. Thus, at a ¹³CH₄/C₃H₆ ratio of 14, *ca.* 70% of the C₄ products were indeed formed by the cross-coupling of CH₄ and C₃H₆. Of the remaining C₄ products, the 20% containing no ¹³C atoms was formed from C₃H₆ alone, while the 11% containing two ¹³C atoms was presumably formed by a more complex set of reactions. It is possible that C₂H₅[•] radicals, derived from ¹³CH₃¹³CH₃, might couple, but this would, of course, give C₄ molecules containing four ¹³C atoms, which were not observed. It is interesting to note that although most of the C₂H₆ product contained two ¹³C atoms, indicating that it was formed primarily from the ¹³CH₄ coupling reaction, the C₂H₄ product contained virtually no ¹³C. Thus, most of the C₂H₄ must have been derived either directly or indirectly from

TABLE 8: Effect of $^{13}\text{CH}_4/\text{C}_3\text{H}_6$ Ratio on ^{13}C Distribution in Products over Li/MgO, (LiCl + NaCl)/MgO, and NaCl-Mn/SiO₂ Catalysts^a

$^{13}\text{CH}_4/\text{C}_3\text{H}_6$	CO _x	percentage of ^{13}C in							
		C ₂ H ₄		C ₂ H ₆		C ₄		C ₆	
		zero ^b	two	zero	two	zero	one	two	zero
Li/MgO									
1.8	7.1	99	0.2	2.2	98	59	38	2.2	
4.4	9.1	98	1.7	2.0	98	44	50	5.6	
9.2	14	92	8.2	1.5	99	30	61	8.9	
14	22	79	22	0.0	100	20	69	11	
(LiCl + NaCl)/MgO									
3.2	3.8	99	1.2	8.3	92	38	62	0.0	100
5.7	15	97	3.5	5.7	94	23	77	0.0	100
11	26	92	7.8	0.0	100	6.2	93	1.0	100
14	29	88	12	0.0	100	2.3	97	1.2	100
NaCl-Mn/SiO ₂									
0.8	5.9	91	9.0	81	19	59	37	3.5	100
3.3	10	89	11	77	23	41	57	2.6	100
5.7	14	87	13	65	35	26	72	2.1	100
9.2	20	74	26	51	49	11	89	0.8	100

^a Reaction temperature = 650 °C; volume of the catalyst = 1 mL; circulation time = 10 min; for the Li/MgO and (LiCl + NaCl)/MgO catalysts $P(\text{CH}_4) = 252$ Torr and $P(\text{O}_2) = 21$ Torr; balance = 10% Ar/helium; for the NaCl-Mn/SiO₂ catalyst $P(\text{CH}_4) = 486$ Torr and $P(\text{O}_2) = 44$ Torr; balance = 10% Ar/helium. ^b Zero, one, and two indicate the number of atoms per molecule of product.

propylene, rather than from secondary dehydrogenation of the C₂H₆. It should also be noted that, even at high $^{13}\text{CH}_4/\text{C}_3\text{H}_6$ reactant ratios, the observed CO_x product contains relatively little ^{13}C , indicating that it was formed primarily from C₃H₆.

From the results of Table 8 it also is evident that over the (LiCl + NaCl)/MgO catalyst the cross-coupling of CH₄ and C₃H₆ contributes even more to the formation of C₄ products than over the Li/MgO catalyst. At a $^{13}\text{CH}_4/\text{C}_3\text{H}_6$ ratio of 14, 97% of the C₄ molecules contained one ^{13}C atom. A small amount of C₂H₆ was formed, and it again contained almost exclusively two ^{13}C atoms per molecule. These results suggest that methyl radicals tend to cross-couple with allyl radicals rather than react with other methyl radicals. Substantially more C₂H₄ than C₂H₆ was formed, and most of the C₂H₄ molecules contained no ^{13}C atoms. Hence, most of the C₂H₄ was derived not from ethane, but from propylene or from 1,5-hexadiene. Over the (LiCl + NaCl)/MgO catalyst it was possible to detect up to 29% 1,5-hexadiene at a $^{13}\text{CH}_4/\text{C}_3\text{H}_6$ ratio of 3.2, and as expected, the C₆ molecules contained no ^{13}C atoms.

The ^{13}C distribution in the C₄ products obtained over the NaCl-Mn/SiO₂ catalyst was similar to that obtained over the (LiCl + NaCl)/MgO catalyst. Again, at larger $^{13}\text{CH}_4/\text{C}_3\text{H}_6$ ratios, the C₄ molecules mainly had one ^{13}C atom. The ^{13}C distribution in the C₂H₆, however, was significantly different from that observed for the other two catalysts in that over 51% of the C₂H₆ contained no ^{13}C . This result is consistent with the observation that a significant amount of ethane was produced during the oxidation of 1,5-hexadiene over this catalyst.

In order to compare these results with those obtained in the single-pass mode, the conversions and selectivities obtained for three catalysts in the recirculating mode are shown in Table 9. Comparison of the data for the Li/MgO catalyst with those in Table 5 reveals that the CO_x selectivity is greater in the recycle mode, which is not surprising since the hydrocarbon products have more time to react. Nevertheless, at a $^{13}\text{CH}_4/\text{C}_3\text{H}_6$ ratio of ca. 10, the C₄ selectivity only decreased from 37% to 26%, and the C₂ selectivity actually increased. Therefore, the ^{13}C distributions of Table 8 appear to be representative of those that would be obtained in a single-pass flow mode. As a result

TABLE 9: Effect of $^{13}\text{CH}_4/\text{C}_3\text{H}_6$ Ratio on the Distribution of Products over Li/MgO, (LiCl + NaCl)/MgO, and NaCl-Mn/SiO₂ Catalysts^a

$^{13}\text{CH}_4/\text{C}_3\text{H}_6$	conversion, %			selectivity, %				
	C ₃ H ₆	$^{13}\text{CH}_4$	O ₂	CO _x	C ₂ H ₄	C ₂ H ₆	C ₄ ^b	C ₆ ^b
Li/MgO								
1.8	48	5.6	85	67	12	2.4	19	0.0
4.4	54	6.3	84	60	15	4.4	20	0.0
9.2	60	6.7	73	50	15	9.6	26	0.0
14	69	8.1	58	42	15	11	32	0.0
(LiCl + NaCl)/MgO								
3.2	21	4.5	35	34	6.4	0.3	31	29
5.7	25	5.5	35	29	9.2	0.8	38	24
11	38	8.8	27	20	15	2.1	52	11
14	39	8.4	22	17	18	4.2	54	6.8
NaCl-Mn/SiO ₂								
0.8	42	5.1	87	49	14	1.7	23	12
3.3	60	6.7	65	44	15	0.8	38	1.3
5.7	71	7.3	58	34	17	0.3	49	0.7
9.2	81	7.9	47	32	17	0.1	51	0.4

^a Reaction conditions were the same as those in Table 8. ^b C₄ = 1-butene and butadiene; C₆ = 1,5-hexadiene.

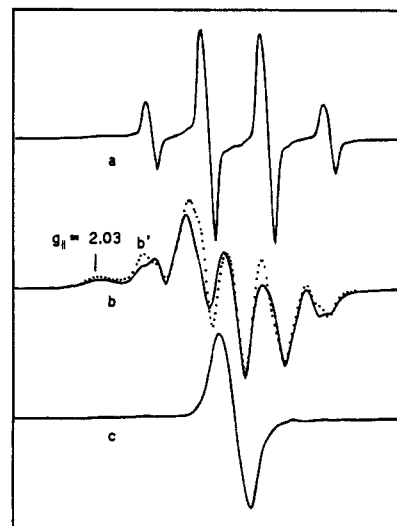


Figure 2. ESR spectra of methyl and allyl radicals: (a) CH₃* radicals formed over Li/MgO, (b) C₃H₅* radicals formed over Li/MgO; (c) C₃H₅* radicals with a small amount of CH₃* formed over (LiCl + NaCl)/MgO; (c) C₃D₅* radicals formed over Li/MgO.

of the longer contact times in the recirculating reactor, no 1,5-hexadiene was observed.

Study of Surface-Generated Gas-Phase Radicals. The MIESR system has been extensively used previously to detect gas phase hydrocarbon radicals that emanate from catalytic surfaces during oxidation reactions.^{20,21} The system was originally designed to detect allyl radicals formed during the oxidation of propylene,¹⁵ although in recent years it has been primarily devoted to the detection of methyl radicals formed during the oxidative coupling of methane. Quantitative studies have shown that the coupling of methyl radicals in the gas phase is a major pathway for the catalytic production of ethane.^{22,23} The role of these surface-generated gas-phase radicals in cross-coupling reactions, however, has not previously been reported.

The ESR spectra of methyl and allyl radicals are compared in Figure 2. The low field maximum at $g_{||} = 2.03$ in the C₃H₅* radical spectrum results from C₃H₅O₂* radicals which are formed in the cooler regions of the system. There is also a component of the peroxy radical spectrum at $g_{\perp} = 2.00$. Methylperoxy radicals have a similar value for $g_{||}$; therefore, it is not possible to distinguish between the two species. The amount of peroxy

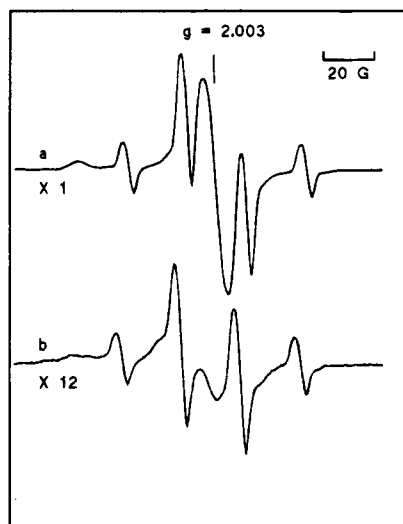


Figure 3. ESR spectra of CH_3^* and C_3D_5^* radicals formed over Li/MgO: (a) with Ar as the matrix gas; (b) with CO_2 as the matrix gas.

radicals could be minimized by increasing the hydrocarbon-to-oxygen ratio, but it was desirable to operate under conditions that were not strictly oxygen limited.

Except for the contribution of the peroxy radical spectrum, the observed C_3H_5^* radical spectrum, obtained with Li/MgO as the catalyst, is in good agreement with a simulated spectrum that was based on g values and hyperfine splitting constants reported in the literature.⁹ Since there is no CH_3^* radical contribution to the spectrum, one can conclude that C–C bonds were not broken over this catalyst. By contrast, a small amount of CH_3^* was formed from C_3H_6 over the (LiCl + NaCl)/MgO catalyst. This is evident from the reversal in amplitude for the outer two peaks, indicated by the dashed line in spectrum b' of Figure 2. Similar evidence for CH_3^* radicals from C_3H_6 was found in the spectrum (not shown) obtained when NaCl–Mn/SiO₂ was the catalyst. The small or negligible amount of CH_3^* produced from C_3H_6 is consistent with the observation (Table 8) that most of the C_2H_6 was derived from CH_4 over the Li/MgO and (LiCl + NaCl)/MgO catalysts. Over the NaCl–Mn/SiO₂ catalyst, much of the C_2H_6 was derived from the cracking of 1,5-hexadiene.

Since CH_3^* and C_3H_5^* radicals have partially overlapping spectra, C_3D_6 was used as the form of propylene when both hydrocarbon reagents were present. The ESR spectrum of C_3D_5^* is shown in Figure 2, spectrum c. The relative concentrations of the CH_3^* and C_3D_5^* radicals were obtained by performing a double integration of the spectra containing only one species. Then the amplitude of a peak in the derivative spectrum was related to this second integral. Using this ratio, it was possible to estimate the relative amounts of each radical from a composite spectrum. Because of the errors involved in this technique, the results are only semiquantitative; nevertheless, they provide evidence for trends that occurred over the catalysts. At the reaction temperatures of interest, a kinetic isotope effect of about 1.5 is expected.²⁴ The relative concentrations have not been corrected for this effect.

We previously demonstrated that CO_2 poisons the active centers for CH_3^* radical formation on the more basic metal oxide catalysts.^{23,25} Thus, any comparison of CH_3^* radical formation at low pressures with the catalytic results obtained at considerably higher pressures must reflect this effect of CO_2 . The comparative results reported here were obtained first with Ar and then with CO_2 as the matrix-forming gas.

In Figure 3 the results obtained over a Li/MgO catalyst, with both Ar and CO_2 as the matrix forming gas, are compared. It is

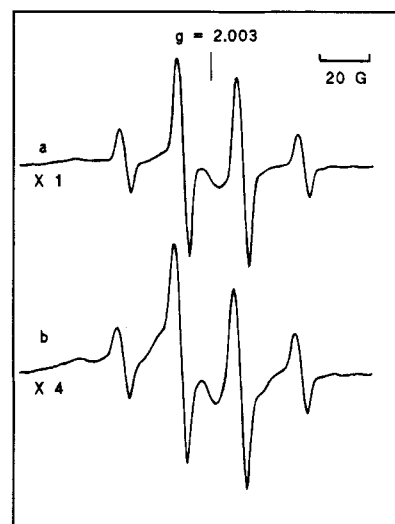


Figure 4. ESR spectra of CH_3^* and C_3D_5^* radicals formed over NaCl–Mn/SiO₂: (a) with Ar as the matrix gas; (b) with CO_2 as the matrix gas.

TABLE 10: Relative Concentrations of Methyl and Allyl Radicals

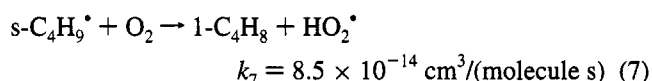
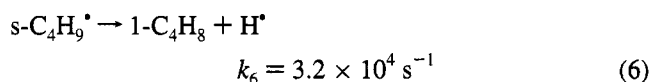
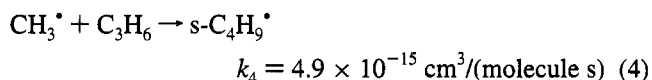
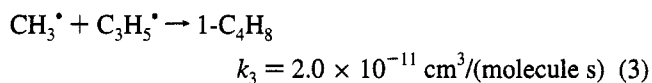
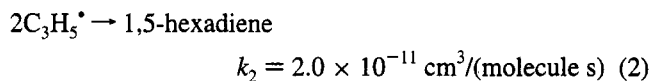
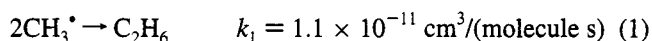
catalyst	Ar matrix		CO_2 matrix	
	C_3D_5^*	CH_3^*	C_3D_5^*	CH_3^*
Sr/La ₂ O ₃	7.1	21	1.5	6.4
Li/MgO	23	6.7	0.4	0.4
(LiCl + NaCl)/MgO	0.7	1.4	0.4	0.9
NaCl–Mn/SiO ₂	1.0	2.2	0.7	1.6

evident that in the presence of CO_2 the total number of radicals formed decreased by more than an order of magnitude. Moreover, CO_2 had a greater poisoning effect on the production of allyl radicals than on the production of methyl radicals. By contrast, as shown in Figure 4, the effect of CO_2 was less dramatic for the NaCl–Mn/SiO₂ catalyst, which might be expected since this is a much less basic catalyst than Li/MgO. In this case, carbon dioxide had about the same poisoning effect on both methyl and allyl radical production.

The relative concentrations of the two types of radicals are summarized in Table 10. In the absence of added CO_2 , Sr/La₂O₃ was the most active catalyst for CH_3^* radical formation, with Li/MgO being the most active for C_3H_5^* radical formation. When CO_2 was used as the matrix-forming gas, all of the catalysts became less effective for the generation of radicals; however, the effect was more dramatic for the strongly basic oxides, Li/MgO and Sr/La₂O₃. Even in the presence of CO_2 , however, the Sr/La₂O₃ remained the best catalyst for radical generation. This is surprising since Sr/La₂O₃ was not a particularly active catalyst for the conversion of CH_4 and C_3H_6 (Table 2). The difference between the MIESR results and the conventional catalytic results may be due to the amounts of CO_2 present in the two types of experiments. In the MIESR experiment, the pressure of CO_2 was about 1 Torr, whereas in the conventional catalytic experiment the pressure of CO_2 over Sr/La₂O₃ was about 22 Torr.

The ratio of allyl-to-methyl radicals is perhaps not obvious from the CO_2 -poisoned spectra of Figures 3 and 4. Because of the larger line width the second integral of the C_3D_5^* spectrum is much larger than is apparent from the amplitude of the derivative spectrum. For each of the catalysts, except Sr/La₂O₃, the $\text{CH}_3^*/\text{C}_3\text{D}_5^*$ ratio was 1–2, but with Sr/La₂O₃ this ratio was greater. In agreement with this observation, the C_2/C_4 product ratio was larger over Sr/La₂O₃ than over the other catalysts (Table 2).

Reaction Mechanism. The presence of both methyl and allyl radicals over the cross-coupling catalysts suggests that both heterogeneous and homogeneous reactions occur during the oxidative conversion of methane and propylene to 1-butene. The gas phase rate constants for the relevant gas phase reactions at 650 °C are^{26–28}



In addition to the coupling and cross-coupling reactions 1–3, one must also consider the formation of 1-C₄H₈ via reactions 4, 6, and 7. If one assumes a reasonable concentration of 1×10^{14} radicals/cm³ for both CH₃[•] and C₃H₅[•],²² then the rate of product formation via reactions 1–3 would be about 1×10^{17} , 2×10^{17} , and 2×10^{17} molecules/(cm³ s) for ethane, 1,5-hexadiene, and 1-butene, respectively. It turns out that the rate of 1-butene formation via the methylation of propylene is small because the s-C₄H₉[•] radicals prefer to revert back to CH₃[•] and C₃H₆ (reaction 5) rather than to lose H[•] (reaction 6) or react with O₂ (reaction 7). At C₃H₆ and O₂ concentrations of 5×10^{17} and 4×10^{17} molecules/cm³, respectively, the relative rates are $r_5/r_6 = 36$ and $r_5/r_7 = 30$. Although the rate of s-C₄H₉[•] formation is 2×10^{17} molecules/(cm³ s), most of these radicals do not react further to produce 1-butene. These approximate results indicate that (i) the methylation of propylene is not a competitive route to the C₄ products and (ii) the production of ethane is expected to be less than that of 1-butene, as was experimentally observed. The rate of 1,5-hexadiene formation is comparable to that of 1-butene formation, but the 1,5-

hexadiene reacts further, as noted in Table 7, to yield mainly propylene at 650 °C.

Conclusions

Of the several catalysts studied, NaCl–Mn/SiO₂ was the most effective for the cross-coupling reaction involving methane and propylene to form 1-butene and butadiene. Experiments utilizing ¹³CH₄ confirm that methane incorporation does indeed occur in this reaction. The simultaneous formation of methyl and allyl radicals over the catalysts suggests that the coupling occurs via a heterogeneous–homogeneous mechanism. The coupling of allyl radicals with each other results in the formation of 1,5-hexadiene, which is unstable under reaction conditions and, to a large extent, converts back to propylene.

Acknowledgment. We acknowledge financial support of this work by the Division of Chemical Sciences, Office of Basic Energy Sciences, U.S. Department of Energy.

References and Notes

- (1) Khcheyan, Kh. E.; Revenko, O. M.; Borisoglebskaya, A. V.; Fishman, D. L. *Zh. Org. Khim.* **1976**, *12*, 467.
- (2) Osada, Y.; Enomoto, K.; Fukushima, T.; Ogasawara, S.; Shikada, T.; Ikariya, T. *J. Chem. Soc., Chem. Commun.* **1989**, 1156.
- (3) Suzuki, T.; Wada, K.; Watanabe, Y. *Appl. Catal.* **1989**, *53*, L19.
- (4) Otsuka, K.; Hatano, M.; Amaya, T. *J. Catal.* **1992**, *137*, 487.
- (5) Kim, H.; Suh, H. M.; Paik, H. *Appl. Catal.* **1992**, *87*, 115.
- (6) Khan, A. Z.; Ruckenstein, E. *J. Catal.* **1993**, *143*, 1.
- (7) Ruckenstein, E.; Khan, A. Z. *J. Catal.* **1994**, *145*, 390.
- (8) Driscoll, D. J.; Lunsford, J. H. *J. Phys. Chem.* **1985**, *89*, 4415.
- (9) Wertz, J. E.; Bolton, J. R. *Electron Spin Resonance*; McGraw-Hill: New York, 1972; pp 118–120.
- (10) Sofranko, J. A.; Leonard, J. J.; Jones, C. A. *J. Catal.* **1987**, *103*, 302.
- (11) Sodesawa, T.; Matsubara, M.; Stahel, S.; Nozaki, F. *Chem. Lett.* **1987**, 1513.
- (12) Lunsford, J. H.; Hinson, P. G.; Rosynek, M. P.; Shi, C.; Xu, M.; Yang, X. *J. Catal.* **1994**, *147*, 301.
- (13) Ruckenstein, E.; Khan, A. Z. *J. Catal.* **1993**, *141*, 628.
- (14) Shi, C.; Rosynek, M. P.; Lunsford, J. H. *J. Phys. Chem.* **1994**, *98*, 8371.
- (15) Martir, W.; Lunsford, J. H. *J. Am. Chem. Soc.* **1981**, *103*, 3728.
- (16) Ito, T.; Wang, J.-X.; Lin, C.-H.; Lunsford, J. H. *J. Am. Chem. Soc.* **1985**, *107*, 5069.
- (17) Mamoun, H.; Robine, A.; Bonnaudet, S.; Cameron, C. J. *Appl. Catal.* **1990**, *58*, 269.
- (18) Burch, R.; Squire, G. D.; Tsang, S. C. *Appl. Catal.* **1988**, *43*, 105.
- (19) Miradotas, C.; Perrichon, V.; Durupt, M. C.; Moral, P. In *Catalyst Deactivation*; Delmon, B., Froment, G. F., Eds.; Elsevier: Amsterdam, 1987; pp 183–195.
- (20) Lunsford, J. H. *Langmuir* **1989**, *5*, 12.
- (21) Driscoll, D. J.; Campbell, K. D.; Lunsford, J. H. *Adv. Catal.* **1987**, *35*, 139.
- (22) Campbell, K. D.; Morales, E.; Lunsford, J. H. *J. Am. Chem. Soc.* **1987**, *109*, 7900.
- (23) Campbell, K. D.; Lunsford, J. H. *J. Phys. Chem.* **1988**, *92*, 5792.
- (24) Driscoll, D. J.; Lunsford, J. H. *J. Phys. Chem.* **1983**, *87*, 301.
- (25) Xu, M.; Shi, C.; Yang, X.; Rosynek, M. P.; Lunsford, J. H. *J. Phys. Chem.* **1992**, *96*, 6395.
- (26) Slagle, I. R.; Gutman, D.; Davies, J. W.; Pilling, M. J. *J. Phys. Chem.* **1988**, *92*, 2455.
- (27) Tsang, W. *J. Phys. Chem. Ref. Data* **1991**, *20*, 221.
- (28) Westley, F.; Herron, J. T.; Cvetanovic, R. J.; Hampson, R. F.; Mallard, G. NIST Chemical Kinetics Database, Version 3.0, National Institute of Standards and Technology, U.S. Department of Commerce, 1991.